The authors would like to thank the editor for their comments on this paper. These comments have been reproduced here in black font color, and author responses are included in red.

Topical Editor Comments for
"Observations of the thermodynamics and kinematic state of the atmospheric boundary layer over the San Luis Valley, CO using remotely piloted aircraft systems during the LAPSE-RATE field campaign"

Comments
Title: The title would be more descriptive and consistent with others in the special issue if it included University of Oklahoma or CopterSonde 2.
This has been modified to include the CopterSonde 2. The title is now: "Observations of the thermodynamic and kinematic state of the atmospheric boundary layer over the San Luis Valley, CO using the CopterSonde 2 remotely piloted aircraft system in support of the LAPSE-RATE field campaign".

line 24: RPAS research at OU since the 1980's is early. Add reference(s) to support this statement.
The authors made their best attempts to find a published reference to this work by Dr. Bergey, however we were unsuccessful. Thus, we have stricken this phrasing from the document.

Grammar/typographical
line 21: plural - "platforms used" included three different aircraft numbers.
Edited as suggested.

line 55: "For this deployment …" should specify LAPSE-RATE after prior sentence with other campaigns. "For the LAPSE-RATE deployment …"
Edited as suggested.

Figure 2. caption: "Aerial" here is awkward. Suggest deleting so caption reads, "Map of the San Luis Valley …"
Edited as suggested.

line 278: link repeats in reference
Edited as suggested.

line 297: link repeats in reference
Edited as suggested.

The authors would like to thank Reviewer 1 for their comments on this paper. These comments have been reproduced here in black font color, and author responses are included in red.

Title: Observations of the thermodynamic and kinematic state of the atmospheric boundary layer over the San Luis Valley, CO using remotely piloted aircraft systems during the LAPSE-RATE field campaign

Summary: The manuscript describes sampling strategies and data collection using remotely piloted aircraft (RPA). Additionally,there are sections on platform inter-comparability, data quality,and processing. Lastly, techniques are described to evaluate the thermodynamic and kinematic state of the atmospheric boundary layer (ABL) over complex terrain with focus on applications for convective initiation, drainage flows, and ABL transitions.

Recommendation: The authors present the results from an interesting and unique field campaign. I recommend publication with minor revisions.

Key points

I suggest reorganizing the manuscript a bit for clarity. Section 4 "Data Processing", comes at the end of the paper but it would strengthen the conclusions in Section 3 "Examples of Flight Data" if Section 4 was moved earlier into Section 2.1 "Description of the CopterSonde". Along this line of thinking I suggest moving Table 4 out of the summary section and showing it earlier in the paper. In the summary it is suggested to include larger implications to the data collection and analysis such as if the datasets collected throughout the six days led to improved forecasts for the San Luis Valley or did the campaign provide an avenue for increased use of RPAs in WMO, NOAA, or NCAR field campaigns? Line 19 of the introduction mentions, "unique opportunity to undertake an intensive comparison of the sensing capabilities of the aerial systems being utilized as a part of the campaign." But the summary does not reiterate the reason this opportunity was unique or its lasting implications.

We agree with the reorganization of the paper. Table 4 is now moved up to section 2 and is now Table 2. The Data Processing section will now come before the case study examples. We have added some text and references to highlight how this data is being used to the summary to solidify the projected impact of this data set. The last paragraph of the introduction has also been reworked to reflect all of the changes to the architecture of the paper.

As for the comment regarding line 19, we have added some text and references to the first introductory paragraph in lines 20-24. We hope this will more easily point readers to information regarding the overall LAPSE-RATE campaign (de Boer et al BAMS 2020) as well as highlight a case study examining the utility of using RPAS data from LAPSE-RATE for forecasting applications (Glasheen et al JAIS 2020, Pinto et al ESSD 2020) and the ESSD paper highlighting the work forecasters did as a part of this effort.

It is nice to see the larger detail in figures 3 and 4 but it would help the reader in the discussion of comparisons if the figures were side by side or closer together.
Figures 3 and 4 were combined into one figure and the caption was changed to reflect the subfigures.

Section 3.2 would be strengthened with more discussion on accuracy and precision of the dataset rather than just listing references so moving Section 4 earlier can address this. Additionally, adding in comparison data on figures from the radiosonde flights, CLAMPS AERI and Doppler LIDAR observations would be beneficial.
Section 4 (data processing) was moved to now precede the data examples as Section 3. Since the AERI and LIDAR data are described in a separate paper, the appropriate citation was added and we chose not to overlay those data here for clarity.

The following suggested changes are to help with clarity;

Line 35-36: Type of sensors (WMO approved)? Moving table 4 up would be helpful here.
The data processing section now comes sooner after this, and references to tables 1 and 4 (now Table 2) were added to direct the reader to the appropriate information. An additional citation was added to Segales et al. (2020) which outlines this aircraft and the sensors used.

Line 44-45: “Section 6 will provide concluding remarks about the dataset as well as future outlooks regarding the future applications of the dataset.” The summary section does not seem to currently include “outlooks regarding the future applications of the dataset.”
Two sentences have been added starting at line 237 to highlight what studies this data set has already been utilized as a part of as well as upcoming papers that will be harnessing this data. We have also restructured this last paragraph of the introduction to point readers to efforts by other LAPSE-RATE teams as well as the overview and intercomparison efforts.

Figure 1 and Line 56: An immediate question for the reader is how the props influence the atmospheric sensors when viewing figure 1 then on line 56 it is mentioned the props were changed. Including a sentence or two on how prop wash has been considered would be helpful to the reader.

We added a comment that changing these propellers should not affect thermodynamic observations (lines 86-88) and also added a citation to Greene et al. (2019), which studied these effects on the same model of CopterSonde.

Line 64-69: Resolution of sensor measurements differ among variables. Moving lines 186 –190 here would be helpful to the reader.
We added the following to lines 79-80: "As will be discussed later, data from the different sensors were interpolated or downsampled so that all observations have a common time vector."

Line 123 –124: Why different ascent and decent rates? Are rates optimized for sensor accuracy accounting for airflow? Was 10s loiter data kept? Did you use separate surface platform measurements to combine the last 10m of descent? Moving lines 199 –208 here would be helpful.
We have added the following at lines 135-139: "As will be discussed in Section 3, only the ascent portion of these vertical profiles are considered for analysis. We therefore chose to fly slower on the ascent to maximize the vertical resolution when accounting for thermodynamic sensor response times. Moreover, by descending more rapidly we are able to achieve a higher maximum profile altitude than we would otherwise with the same battery configuration on the CopterSonde."

Figure 3: The significant digits on the temperature contours seem to imply a measurement precision that is contradicted in table 4.
This was an artifact of creating the figures in Python. The number of significant figures have been reduced to reflect the accuracy of the measurements.

Line 136 –137: It is mentioned that flight frequency changed between 15min and 30 min for MOFF site but figures 3 and 4 both show changing flight frequency depending on time of day. It would be helpful to describe why flight frequency changed at particular times. For example, there is an hour between flights on Figure 3 (1500 –1600) and there is an increase in flight frequency on Figure 4 from 1830 –1944.
The sentence was reworded to reflect when the flight frequency at MOFF changed and why. A sentence was added at ~line 195 was added to explain why the flight frequency increased after 1830 UTC at both sites.

Line 141: "Figure 3 also shows the post convection cool down around 1800 UTC." This cool down is difficult to discern in the figure given the changing temperature contour separations and not knowing measurement precision (unless table 4 is moved earlier). It could help the reader to give actual temperature values or ranges to strengthen this observation.

Two sentences were added (lines 200-204) were added to clarify the observed temperature difference. It will also help that the two figures are now next to each other.

Line 154 –155: “While a small bias between the two aircraft exists in temperature. . .” At the surface and at 600m this looks to be almost 2 degrees which may not be small given the claim of a post convection cool down in figure 3. For all the graphs, does showing error bars make the graphs too difficult to read? Having the error bars could support the claim that the biases are small and winds show reasonable agreement.
This is an interesting observation and we agree that additional context is warranted. The following was added in lines 231-241: In our experience with the CopterSonde, the discrepancies in the temperatures between the two identical platforms can be attributed to three main sources: 1) sunlight on an inadequately shielded sensor (discussed in Greene et al. 2019) at the correct relative angles of aircraft heading and sun zenith/azimuth; 2) natural variability in the atmosphere -- the 2 aircraft were 10-20 m apart, so this is not entirely unreasonable for a convective boundary layer; and/or 3) systemic bias related to calibration of the CopterSonde thermodynamic sensor package as a whole. While a combination of these three is the most likely explanation, we believe the spatial/temporal heterogeneity of the atmosphere during these observations should not be overlooked. For example, 3-second sonic anemometer temperatures from the Bailey et al. 2020 ESSD paper for this campaign reveal that during the 10-minute timeframe during these concurrent CopterSonde profiles (albeit at a different site but featuring similar land cover properties), 2-meter temperatures fluctuated by up to 4°C. Doppler lidar observed vertical velocities collocated with the CopterSondes (Bell et al. 2020a,b) also indicate ~3 m/s updrafts at the same time as the profile in this figure. Turbulent transport of temperature therefore likely contributed to large spatial and temporal heterogeneity that can be detectable at the 10 - 20 m separation scales in this particular comparison flight.

While further investigation into the relative contributions of these differences is beyond the scope of this paper, the context outlined above has been added for clarity. Here we also choose not to include error bounds, as the +/-0.5 °C accuracy from Table 4 (now Table 2) does not explicitly incorporate the effects of the spatial heterogeneity impacting the comparison of these two profiles that future studies may be interested in examining.

Line 157: While it is helpful to have references on the accuracy and precision of the dataset, it is recommended the authors address this issue in at least a paragraph to support the claims of the inter-comparison flights similar to the explanations given in section 4 Data Processing.
The “Data Processing” section has been moved forward to now be Section 3, so the following details have been added at the end of this section (lines 180-187): “In an effort to quantify the CopterSonde thermodynamic and kinematic observational biases relative

to a ubiquitous standard, Bell et al (2020a) compared vertical profile CopterSonde flights from LAPSE-RATE and in Oklahoma to collocated Vaisala RS92-SGP radiosondes. While unable to explicitly account for factors such as horizontal heterogeneity, the sample ranges in temperature, dewpoint temperature, and horizontal winds were large enough to determine baseline accuracies in each (Table 2). Namely, CopterSonde temperatures were within 0.5 °C of the radiosondes in the aggregate, which is largely due in part to the considerations taken for temperature sensor placement on-board the CopterSonde (Greene et al, 2018, 2019). Additionally, a broad intercomparison effort during the LAPSE-RATE campaign (Barbieri et al, 2019) resulted in similar statistics when comparing the CopterSonde observations to a common mobile meteorological reference."

Line 165: Please give the time for local sunrise.
Edited as suggested.

Line 230: "intercomparibl ity"is misspelled. Intercomparability
Edited as suggested.

The authors would like to thank Reviewer 2 for their comments on this paper. These comments have been reproduced here in black font color, and author responses are included in red.

The authors have a great dataset illustrating phenomena in the boundary layer as measured by a RPAS. I would like to see a rewrite with more emphasis on that aspect as opposed to it reading like a data report see some examples below.

Line 20 This reads more like a data report or experimental field notes than an article on the uniqueness of RPAS for scientific discovery.
Earth System Science Data is a journal that focuses on the dissemination of information about original datasets so that the data can be used by the broader scientific community, rather than the interpretation of these results. The authors believe that this article honors that spirit and was not meant to be an article on the novelty of using RPAS for scientific discovery. It very much is our field notes so that people can understand the strengths and limitations of our dataset.

Line 55 Is it important to know that the carbon fiber blades were switched out??
Yes, because it is an alteration of the platform's typical operating conditions that we have used or will use in other deployments of the CopterSonde RPAS. However, we have made the importance of this clearer based on this remark and feedback contained in the Open Discussion comments in lines 63-66.

Line 185 Why do we need to know that binary data was converted to JSON to CSV??
This information is relevant because the JSON format allows for the varying sampling rates for each data stream to coexist in the same file, whereas the conversion to CSV with a common time vector markedly simplifies reading and processing the data at this stage. This has been emphasized in the text in lines 149-154.

Figure 3 Temperature contours are plotted to the nearest .001 ^{0}C. I highly doubt that the authors have that kind of accuracy and if they do not the resolution of that parameterized back to the accuracy or precision. Figure 5 would indicate that the precision is ~10C. Table 4 would indicate +- 0.5 ^{0}C
For Figures 3 and 4, the contours appearing like they had an accuracy of 0.001 was actually an artifact of the plotting script. This has been corrected to reflect the correct accuracies as specified in Table 4 (now Table 2).

Figure 5 would indicate that the precision is □ 1 0C. Table 4 would indicate +- 0.5 0C
Figure 5 (now Figure 4) has been updated so that the minor tick marks for temperature are every 0.5 °C to be closer to the posted accuracy in Table 4 (now Table 2).

The authors would like to thank Reviewer 3 for their comments on this paper. These comments have been reproduced here in black font color, and author responses are included in red.

summary: The authors describe measurements of the CopterSonde 2 remotely piloted aircraft systems (RPAS) over complex terrain in the San Luis Valley, Colorado. TheCopterSonde 2 and the flight strategy is briefly described, the data processing, availability and quality are discussed. The operations focused on convection initiation studies, diurnal transition studies, internal comparison flights and cold air drainage flows.Coordinated flights shell provide insight into the horizontal heterogeneity. The data set,as a part of the LAPSE-RATE campaign is publicly available.

general remarks: The introduction should explain the scientific goals of the LAPSE-RATE field campaign into more detail. Choice of location, previous measurements on the sight, typical and/or seasonal conditions, wind speeds and direction in this com-plex terrain with regard to synoptic conditions and so on. Further, the applied remote sensing techniques and the other measurement efforts during the campaign should be outlined in the introduction. A global overview of RPAS efforts for ABL studies should be given, rather than highlighting only OU's efforts in the field. The data processing chapter (4) should be moved to the description of the RPAS in Chapter 2 and the Data availability could be mentioned in Flight Strategies (2.2) alongside table 3, for example.The whole section 3 should be strengthened with more plots and details, comparisons to other measurement systems and further evaluations of the described atmospheric thermodynamic and kinematic state.
We have added additional clarification regarding the efforts and remote/in situ instrumentation that supplemented the RPAS data. We agree with the restructuring of the order of sections and have moved the data processing section to be Section 3. As this is an overview of OU's contribution to the campaign, we do not believe it is appropriate to provide a review of the state of the science in this article or detail the other institutions advancements. We have added additional citations to point to our collaborator's efforts in this campaign (lines 51-53) as well as direct interested parties to existing comprehensive reviews on the utilization of RPAS in weather and atmospheric science (lines 24-26).

We believe that providing additional plots and analysis is outside the scope of this article as it is meant to present the data set, discuss how it was collected, and how it can be utilized by other parties. Further analysis on these topics is forthcoming in Lappin et al 2021 and other planned publications.

specific comments:

L6 ff: The data from these coordinated flights provides insight into the horizontal heterogeneity of the atmospheric state over complex terrain as well as the expected horizontal footprint of RPAS profiles. What is meant with footprint? Footprint of the RPAS is confusing.

We agree that footprint is confusing here. We have deleted this phrasing from the sentence and have left the first half of the sentence to highlight how data from all teams could be utilized to highlight variations across the valley.

L18: What kind of conventional remote sensing techniques were applied?

Radiosondes, mobile mesonet units, CLAMPS, and LIDARs were all utilized as a part of the ground based in situ and remote sensing techniques that complimented the RPAS data collected by the participating institutions. That data will be presented in another publication in this special issue, Bell et al (2020b). The reference in the text has been clarified to include both remote and in situ sampling as well as point to this reference, around line 18.

L21: What are the scientific objectives?

As mentioned in lines 17-18 of the previous version, the objective of the campaign was to collect “targeted observations of cold air drainage flows, convection initiation, and morning boundary layer transitions” with RPAS, in situ, and remote sensing instruments. We have rephrased lines 14-20 and added to lines 38-40 to further clarify the campaign's objectives and how we contributed to them.

We have also added additional citations to direct readers to the campaign overview papers in the special issue and the Bulletin of the American Meteorological Society in lines 50-51.

L24-34: What about similar efforts of other institutions?

As this work focuses on OU’s efforts to the campaigns, we will not be discussing our partner institutions here. However, we have added references to these teams’ efforts that are also presented in this special issue in starting at line 51 to assist readers in finding this material.

Figure 1: Does the manuscript include any data of that tower?

No, because this is a photo taken back at our field laboratory in Washington, OK to showcase the RPAS. The data was collected in CO.

L64: Why is Table 4 in the very end and where are the accuracies coming from? What is meant by indirectly?

Table 4 has been brought to Section 2.1 and is now Table 2. The original thinking was that this table is the culmination of the processing and shows explicitly what users will find in the data files, but we acknowledge that this information is useful much more early on in the manuscript. The accuracies originate from the Bell et al. (2020a) study cited in the caption as compared to Vaisala RS92-SGP radiosondes. The “indirectly” comment has been removed for clarity.

L64/L68/L69: Measurements at 10 and 20 Hz should be shown with a spectral analysis. Do the sensor resolve fluctuations that fast? Please provide spectra of an ascend ofthe copter to further discuss the resolution of the sensors.
As described in Section 3, the thermodynamic and kinematic observations are averaged to 3 m altitude bins, which effectively removes the spectral information at the original sampled frequencies. Spectral analysis of these sensors is therefore out of the scope of this data overview paper.

L103-118: Is this section needed?
Yes - it is important to outline how one gets authorization to operate in the National Airspace for people wishing to conduct RPAS work in the future. This is a very important part of collecting the data and may not be obvious to individuals wishing to work with RPAS in the future.

Figure 3 and Figure 4 should be next to each other
Figure 3 and 4 have been combined into one figure.

L137-143: Vague explanations. Please provide further details of how, where and when the feature of interest occur and why this implies the location of CI.
This topic is further investigated in an Atmospheric Measurement Techniques paper, currently in preparation. Commentary about the motivations and methods in the upcoming paper were added in lines 206-209.

Section 3.2: The comparison should include other measurement systems like remote sensing devices, that were on sight. Further, the wind speed is too low in order to compare something. Both systems show unusual wind speed profiles, that do not agree. Maybe not much related to wind speed at all, but to attitude control parameters of the pixhawk autopilot system. Also the wind direction should be shown. Furthercomparison is needed, otherwise this section is not useful.
Because this paper specifically discusses the CopterSonde data collected during LAPSE-RATE, we intentionally chose not to include comparisons to other instruments; however, we have added citations to accompanying datasets in this section. As for the wind profiles, we agree that the comparison presented is not a perfect agreement. We have added a

profile of wind direction to Figure 4d. While deeper discussion into the mechanisms behind the possible disagreement is beyond the scope of this data paper, the following context has been added about how winds are derived (lines 234-241): “As discussed previously, the CopterSonde estimates horizontal wind speeds and directions based on a second-order least-squares regression fit between the aircraft's tilt angle into the wind (calculated from three-dimensional Euler rotation matrices) and an Oklahoma Mesonet 10 m wind reference (Greene et al. 2018, Segales et al. 2020). As more sophisticated autopilot-based adaptive wind estimation techniques become available, future studies should leverage this particular dataset along with other ground-based sensors (Bell et al. 2020b) or large eddy simulations (Pinto et al. 2020) to examine the effects of spatial and temporal heterogeneity on instruments located less than 100 m apart.”

Section 3.3: Please provide further information. Time of sunrise and so on.
Local sunrise time in MDT has been added as suggested.

L167 ff:Surface-based vertical mixing, above 300 m relatively steady-state for most of the early growth and entrainment-based heating of the growing ABL are only very briefly derived and need further
Further discussion and analysis is beyond the scope of this paper, whose primary purpose is just to demonstrate the type of data included in this dataset.

Figure 6 and Figure 7: It would be helpful to mark the features in the graphs and provide further data and graphs of the phenomena under discussion.
These figures have been updated with larger font size and annotations.

Section 3.4: Please provide further data and plots. What about wind speed and direction during this period?
We have added a figure summarizing the wind speed and direction profiles during this timeframe. This is now Figure 7.

L208: averaging intervals and time constants are fundamental. Why is it 1 s? Please provide further details and analysis.
The following details have been added (lines 173-179): “Finally, the 3 m averaging interval was chosen under consideration of the average ascent rate (3 m/s) and an approximate time constant of the sensor payload of 2 s. This time constant is based upon experiments during the ISOBAR18 campaign with an older version of the CopterSonde and identical sensors (Kral et al., 2020; Greene et al., 2021, in preparation) where the aircraft was subjected to a series of quasi-step-function inputs between a sauna and the below-freezing environment of Hailuoto, Finland. The averaging interval of 3 m is therefore

approximately double the vertical resolution as predicted by the response time and ascent rate, so further studies will be needed to elucidate the impacts of these decisions."

L210: subjectively omitted? By hand? Algorithms should detect outliers systematically
We agree, and this is an ongoing effort to automate an objective process. With only 3 T and 3 RH sensors and no true "reference" for each vertical profile aside from a ground station (only occasionally), it is not always possible to determine a "most correct" sensor based just on simple statistics like mean and standard deviation. Therefore, our current method requires subjective inspection of each profile to determine which sensors perform the most similarly (i.e., highly correlate together). Usually there is high correlation and low spread, but occasionally the sensors strongly correlate but are separated by a large offset; other times, sensors weakly correlate but have a small offset. Since we have thus far been unable to determine objective thresholds for these features, a subjective perspective is required. This is the same technique in data processing for the vertical profiles compared in Bell et al. 2020a, which identified accuracies of +/-0.5 °C in temperature and +/-2% RH when compared to Vaisala RS92-SGP radiosondes often regarded as a "gold standard". We are therefore confident in this approach, although we do agree that more explanation is warranted.

Lines 180-185 now read as follows: "Because the CopterSondes were outfitted with 3 temperature and 3 RH sensors each, it was necessary to inspect each of their time-series outputs with respect to one another to determine potential outliers. Although an objective method of doing so is ideal, research into this is still ongoing and thus we chose to subjectively analyze each sensor individually. A given sensor was omitted from further consideration if it did not correlate with the other sensors and/or there was a large bias between them (greater than 0.5 °C)."

Observations of the thermodynamic and kinematic state of the atmospheric boundary layer over the San Luis Valley, CO using the CopterSonde 2 remotely piloted aircraft ~~systems during~~ system in support of the LAPSE-RATE field campaign

Elizabeth A. Pillar-Little[1,2], Brian R. Greene[1,2,3], Francesca M. Lappin[1,2], Tyler M. Bell[1,2,4,5], Antonio R. Segales[2,3,6], Gustavo Britto Hupsel de Azevedo[2,6], William Doyle[2], Sai Teja Kanneganti[2,7], Daniel D. Tripp[4,5], and Phillip B. Chilson[1,2,3]

[1]School of Meteorology, University of Oklahoma, Norman, OK 73072, USA
[2]Center for Autonomous Sensing and Sampling, University of Oklahoma, Norman, OK 73072, USA
[3]Advanced Radar Research Center, University of Oklahoma, Norman, OK 73019, USA
[4]Cooperative Institute for Mesoscale Meteorological Studies, University of Oklahoma, Norman, OK 73072, USA
[5]NOAA/OAR National Severe Storms Laboratory, Norman, OK 73072, USA
[6]School of Electrical and Computer Engineering, University of Oklahoma, Norman, OK 73019, USA
[7]School of Computer Science, University of Oklahoma, Norman, OK 73019, USA

Correspondence: Elizabeth A. Pillar-Little (epillarlittle@ou.edu)

Abstract. In July 2018, the University of Oklahoma deployed three CopterSonde ~~2~~ remotely piloted aircraft systems (RPAS) to take measurements of the evolving thermodynamic and kinematic state of the atmospheric boundary layer (ABL) over complex terrain in the San Luis Valley, Colorado. A total of 180 flights were completed over five days, with teams operating simultaneously at two different sites in the northern half of the valley. Two days of operations focused on convection initiation studies, one day focused on ABL diurnal transition studies, one day focused on internal comparison flights, and the last day of operations focused on cold air drainage flows. The data from these coordinated flights provides insight into the horizontal heterogeneity of the atmospheric state over complex terrain~~as well as the expected horizontal footprint of RPAS profiles. This data set~~. This dataset, along with others collected by other universities and institutions as a part of the LAPSE-RATE campaign, have been submitted to Zenodo (Greene et al., 2020) for free and open access (DOI:10.5281/zenodo.3737087).

1 Introduction

Researchers from the University of Oklahoma (OU) joined colleagues from across the world to take part in the Lower Atmospheric Profiling Studies at Elevation – a Remotely-piloted Aircraft Team Experiment (LAPSE-RATE) campaign during ~~July~~ 13-19 ~~,~~ July 2018 in the San Luis Valley of Colorado. ~~During this campaign , teams~~ This campaign brought teams together from several universities ~~in the United States and Europe partnered with research scientists~~ with researchers from government laboratories such as the National Center for Atmospheric Research (NCAR), National Severe Storms Laboratory (NSSL) and National Oceanic and Atmospheric Administration (NOAA) to conduct targeted observations ~~of cold air~~ to examine five scientific objectives: 1) valley drainage flows, 2) convection initiation, ~~and~~ 3) aerosol properties, 4) turbulence profiling, and 5) morning boundary layer transitions with both ~~conventional remote sensors~~ remote (LIDARs, AERI, radiometer) and in situ (radiosondes, Mobile Mesonet) sensors (Bell et al., 2020b; de Boer et al., 2020c) as well as remotely piloted aircraft systems (RPAS, also commonly referred to as uncrewed aircraft systems, UAS). Additionally, the colocation of so many teams with diverse systems provided a unique opportunity to undertake an intensive comparison of the sensing capabilities of the aerial systems being utilized as a part of the campaign ~~. This manuscript will focus on the data collected by OU in support of the scientific objectives~~ (de Boer et al., 2020b; Barbieri et al., 2019). It also provided an opportunity to assess the accuracy of weather forecasts that were provided by NCAR to the team as a part of the campaign ~~, including the platform used, the data acquisition methods, and the processing and archival process. For details regarding OU's contribution to the sensor intercomparison efforts, readers are directed to Barbieri et al. (2019).~~

~~Research in RPAS~~ (Glasheen et al., 2020; Pinto et al., 2020).

The use of RPAS in the atmospheric sciences has increased significantly with the explosive growth of technologies that are both economical and more user-friendly than previous generations of uncrewed systems (Elston et al., 2015; Brosy et al., 2017; Koch et al., . Research utilizing RPAS for weather applications at OU has been ongoing since ~~the 1980s. However, this work entered a new phase in~~ 2009~~when researchers in the OU~~ , when scientists in the School of Meteorology began exploring ways of utilizing RPAS to take highly resolved profiles of atmospheric state variables (Bonin et al., 2013, 2012), turbulence (Wainwright et al., 2015; Bonin et al., 2015), and ozone (Zielke, 2011) among other phenomena to better understand the evolution and structure of the atmospheric boundary layer (ABL). In 2016, these studies expanded to encompass sensor placement and measurement optimization (Greene et al., 2018), system design and evaluation (Segales et al., 2020a), and sensor integration (Greene et al., 2019) due in large part to the CLOUD-MAP project which facilitated the development of RPAS for the explicit purpose of conducting atmospheric measurements (Jacob et al., 2018). The capabilities of these weather-sensing RPAS ~~(WxRPAS)~~ have been demonstrated in a variety of collaborative field campaigns (de Boer et al., 2019; Jacob et al., 2018; Koch et al., 2018; Kral et al., 2020), calibration and validation experiments (Barbieri et al., 2019), and careful comparison against other remote sensing networks (Bell et al., 2020a).

OU deployed three CopterSonde ~~2 quadcopter RPAS~~ quadcopter RPAS (Segales et al., 2020a) as a part of the LAPSE-RATE campaign. This system ~~measures pressure, temperature, humidity, horizontal wind speed, and horizontal wind direction and~~ successfully captured vertical profiles of these variables up to 914 m above ground level (AGL) during this week-long mission through direct (pressure, temperature, and humidity) and indirect (wind speed and wind direction) measurements (see Tables 1 and 2 for technical specifications). These platforms were deployed to three different sites over the course of the field campaign, typically measuring at two sites simultaneously. This approach resulted in the OU team completing 180 flights that produced quality observational data supporting three of the five campaign objectives (boundary layer transitions, drainage flows, and convection initiation).

This ~~paper describes the data set collected by the OU CopterSonde 2 RPAS during LAPSE-RATE~~manuscript will focus on the data collected by OU in support of the scientific objectives of the campaign, including the platforms used, the data acquisition methods, and the processing and archival process. Section 2 will briefly describe the CopterSonde ~~2~~ RPAS as well as the operational strategy for this field campaign. Section 3 will ~~highlight some examples of data products available within this data set, while Section 4 will~~ discuss the data logging, processing, and quality control procedures, while Section 4 will highlight some examples of data products available within this dataset. Section 5 will outline the format, location, and associated metadata of the publicly available dataset. Finally, Section 6 will provide concluding remarks ~~about the dataset as well as~~ as future outlooks regarding the future applications of the ~~data set.~~ dataset. For details regarding OU's contribution to the sensor intercomparison efforts, readers are directed to Barbieri et al. (2019). More information regarding the overall campaign such as information surrounding the synoptic conditions, community engagement efforts, and campaign objectives can be found in de Boer et al. (2020a) and de Boer et al. (2020b). Finally, material outlining the contribution of the other participating institutions can be found in this special issue (Bailey et al., 2020; Bell et al., 2020b; Brus et al., 2020; de Boer et al., 2020c; Pinto et al., 202
.

2 Description of the CopterSonde RPAS and Flight Strategy

2.1 CopterSonde ~~2~~ RPAS

The RPAS utilized for this field campaign was the CopterSonde 2 (hereinafter, CopterSonde) (Figure 1; see Segales et al., 2020a), which was designed and manufactured by the Center for Autonomous Sensing and Sampling (CASS) at ~~the University of Oklahoma~~OU. The CopterSonde ~~2~~ is a rotary-wing platform that is based on a modified version of the Lynxmotion HQuad500 wide-X type quadcopter with fixed-pitch rotors that has been optimized for vertical profiling operations. The CopterSonde's technical specifications can be found in Table 1. Additional information regarding the design and development of the CopterSonde series is described in Segales et al. (2020a). The CopterSonde RPAS has been proven to be capable of collecting thermodynamic and kinematic profiles of the atmosphere in a variety of environments from summer in the Southern Great Plains in pre-convective environments (Koch et al., 2018) to polar winter conditions in the ~~Artic~~ Arctic (Kral et al., 2020). For ~~this~~ the LAPSE-RATE deployment, the CopterSonde ~~2~~ was piloted under its typical operating parameters except its standard 11" x 5.5" T-style carbon fiber propellers were swapped for a 12" x 5" model to increase the maximum thrust of the vehicle required to overcome the ~~higher~~ high density altitude in south central Colorado ~~.~~ resulting from warm temperatures and high altitudes above mean sea level (MSL). Because the thermodynamic sensors are mounted inside a fan-aspirated L-duct on the front end of the aircraft, results from Greene et al. (2019) indicate that changing the propellers should not affect the quality of thermodynamic observations. All the CopterSonde's flights during the campaign were done in a semi-autonomous mode, meaning that the platform flew a pre-programmed mission and was only manually controlled by the operator during ~~take-off and~~ landing. Commands were sent to the RPAS over a telemetry link and data collected were streamed back to the ground station where they were displayed on a customized interface that allowed for real-time monitoring. The ground station and RPAS communicated via a 900 MHz Radio (RFD 900+, RFD Design) that has a range of 40 km.

Figure 1. Photograph of the OU CopterSonde RPAS (Norman, OK, USA) in flight next to an experimental 10 m flux tower.

~~The CopterSonde 2~~

The CopterSonde is outfitted with sensors that enable it to measure atmospheric state variables as it ascends along its flight path (see Table 2 for details). The wind speed and wind direction were calculated ~~indirectly~~ at 10 Hz using the Wind Vane Mode algorithm described in Segales et al. (2020a) which utilizes the roll, pitch, and yaw angles measured with the inertial measurement unit (IMU) on-board the RPAS's autopilot system, the Pixhawk CubeBlack. The pressure was measured at 10 Hz with a MS561 capacitive pressure sensor inside the Pixhawk CubeBlack, which is also utilized for altitude. Atmospheric temperature was measured at 20 Hz with a fast response bead thermistor (International Met Systems). Relative humidity was measured at 10 Hz using the HYT 271 capacitive humidity sensor (Innovative Sensor Technologies). As will be discussed later, data from the different sensors were interpolated or downsampled so that all observations have a common time vector. The temperature and humidity sensors were enclosed in a custom sensor scoop that was 3D printed out of polylactic acid (PLA). The sensors were located inside the tubular portion of an L-shaped duct and were mounted in an inverted V configuration. At the base of the duct was a smart fan that was programmed to aspirate the sensors at a rate of 12 m s^{-1} and was toggled on ~~and off~~ during ascent at a height of 1.85 m AGL and off during descent at a height of ~~1.85 m~~ 1.45 m AGL to prevent dust and debris from being pulled into the scoop. Each scoop ~~constructed~~ was distinguished utilizing ~~a~~ an identification code and calibrated

Table 1. Technical Specifications of the OU CopterSonde

Frame size	500 mm
All-up weight	2.25 – 2.36 kg
Maximum speed	$26.4\ \mathrm{m\ s^{-1}}$
Maximum ascent rate	$12.2\ \mathrm{m\ s^{-1}}$
Maximum descent rate	$6.5\ \mathrm{m\ s^{-1}}$
Maximum altitude above ground[a]	1800 m
Maximum altitude above sea level	3050 m
Maximum wind speed tolerance	$22\ \mathrm{m\ s^{-1}}$
Flight endurance[a]	18.5 min
Operating temperatures[b]	-20 °C – 40 °C
Measured Thermodynamic Variables	Temperature, Pressure, Relative Humidity
~~Measured~~ Derived Kinematic Variables	Wind Speed, Wind Direction

[a] under favorable weather conditions with low winds.

[b] tested temperatures, the range can be larger than stated.

Table 2. Description of the thermodynamic and kinematic parameters available in each CopterSonde data file. Also includes information on the method each parameter was measured along with their relative accuracies based on Bell et al. (2020a) compared to Vaisala RS92-SGP radiosondes.

Parameter	**Method**	**System Accuracy**
Temperature	3 iMet-XF Bead Thermistors	±0.5°C
Relative Humidity	3 IST HYT-271 Capacative Hygrometers Converted to dewpoint temperature then recalculated using (relatively) fast-response iMet-XF bead thermistors	±2%
Dewpoint Temperature	Converted from temperature and relative humidity measured by the 3 IST HYT-271 sensors	±0.5°C
Pressure	TE MS5611 Barometric Pressure Sensor (inside Pixhawk 2.1 Autopilot)	±1.5 hPa
Wind Speed	Linear regression of tilt angles compared to reference	$\pm 0.6\ \mathrm{m\ s^{-1}}$
Wind Direction	Linear regression of tilt angles compared to reference	±4°

prior to the field campaign using the procedure outlined in Greene et al. (2019). Further information regarding considerations for sensor placement, aspiration, and shielding on the CopterSonde ~~RPAS~~ can be found in Greene et al. (2018, 2019). More on the data quality and statistical performances will be discussed in Section 3.

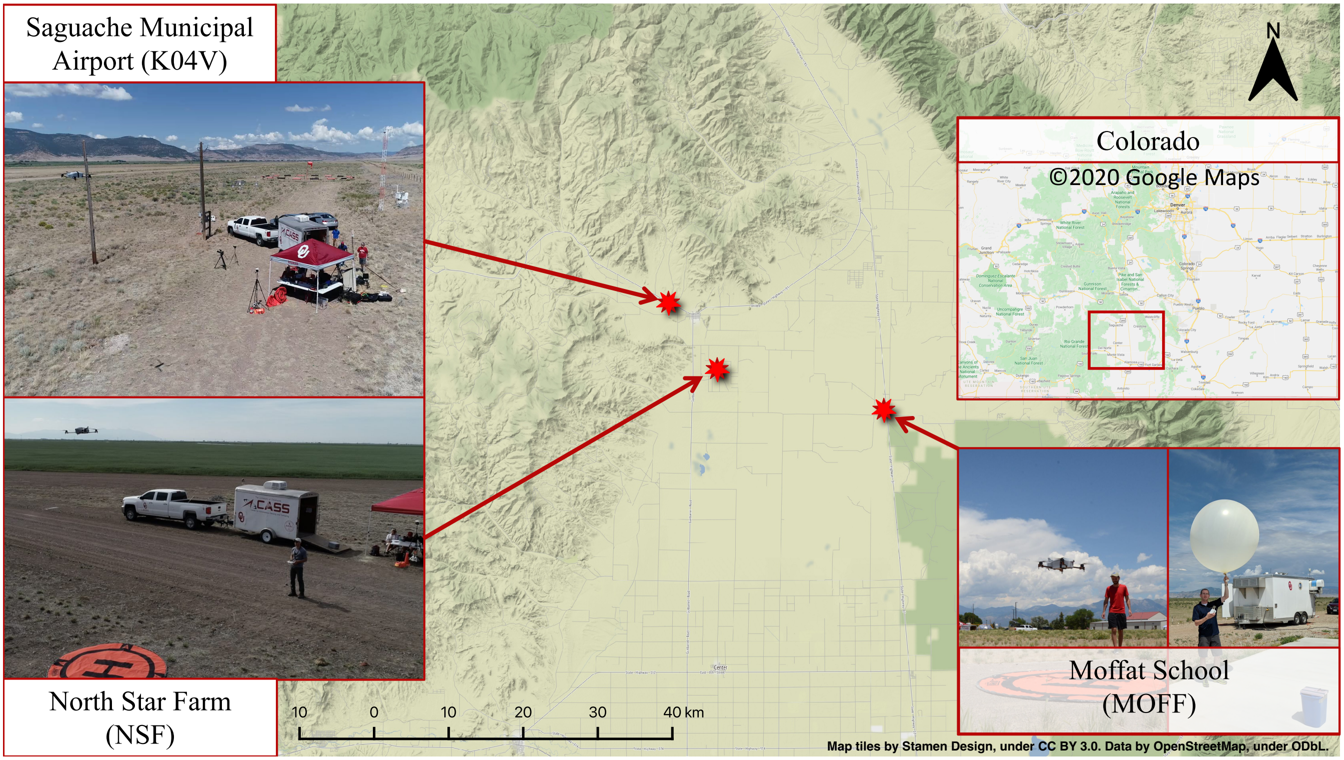

Figure 2. ~~Aerial map~~ Map of the San Luis Valley in south-central Colorado (data ©2020 OpenStreetMap), with CASS deployment locations denoted by the red stars. Inset images beginning from the top left and moving counterclockwise: Saguache Municipal Airport (K04V, photo credit William Doyle), North Star Farm (NSF, photo credit William Doyle), Moffat School (MOFF, photo credit Tyler Bell), and a map of the state of Colorado with the San Luis Valley outlined in red (courtesy Google Maps, ©2020).

2.2 Flight Strategies

The LAPSE-RATE campaign featured five unique scientific objectives: morning atmospheric boundary layer transitions, aerosol properties, valley drainage flows, deep convection initiation, and atmospheric turbulence profiling. Each evening, the individual LAPSE-RATE teams would gather for a weather briefing and discuss which objectives would be the most advantageous to target based on forecasts prepared by NCAR scientists. Teams would then distribute themselves across the San Luis Valley to best sample the phenomena of interest. For more detailed information about the overall campaign goals, science objectives, synoptic and mesoscale conditions driving the selection of objectives, please see the LAPSE-RATE overview article in this special issue (de Boer et al., 2020b).

The CopterSonde was deployed at three different locations across the San Luis Valley in support of LAPSE-RATE scientific objectives. These locations were ~~Moffat Consolidated School (MOFF),~~ Saguache Municipal Airport (K04V), Moffat Consolidated School (MOFF), and the southern edge of North Star Farms (NSF). Latitude and longitudes of these deployment locations as well as their altitude above mean sea level (m MSL) are summarized in Table 3. A visual representation of these

Table 3. List of sites during LAPSE-RATE where CASS operated.

Site (Abbreviation)	Latitude (°N)	Longitude (°E)	Altitude (m MSL)
Saguache Municipal Airfield (K04V)	38.099156	-106.171331	2385.2
Moffat School (MOFF)	37.997587	-105.911795	2305.6
North Star Farm (NSF)	38.036093	-106.112658	2330.8

locations with respect to the layout of the valley is provided in Figure 2, with the inset focusing on the layout of the multiple assets operating at MOFF. The MOFF and NSF sites were both located in the central portion of the valley whereas K04V was situated in a narrowing section of the valley with steeper valley walls to the northwest of NSF. ~~MOFF and~~ K04V and MOFF were dominated by scrublands while NSF was primarily comprised of irrigated cropland.

OU deployed a team daily to MOFF regardless of objective due to the colocation of the Collaborative Lower Atmosphere Mobile Profiling Station (CLAMPS) at the site. Not only did this create a local supersite in the central region of the valley, it facilitated the intercomparison of the RPAS with more conventional instrumentation such as radiosondes, atmospheric emitted radiance interferometer (AERI), microwave radiometer (MWR), and Doppler LIDAR (Bell et al., 2020a; Wagner et al., 2019). A second OU team was deployed to one of three locations depending on the daily objective. For the convection initiation (CI) and boundary layer transition (BLT) study days, the second team set up at K04V. For the cold air drainage study, the team deployed to NSF. Across all three sites, 180 successful flights were completed in support of LAPSE-RATE. Details regarding the number of flights per day, daily science objectives, start and stop times, and specific vehicles used are summarized in Table 3.

All flights completed by OU as a part of LAPSE-RATE were conducted either under Federal Aviation Authority (FAA) Part 107 regulations or under the Oklahoma State University's FAA Certificate of Authority (COA) 2018-WSA-1542 effective from ~~July~~ 13 ~~to July~~ - 22 ~~,~~ July 2018. This COA permitted daytime operations of small RPAS weighting less than 25 kg (55 lbs.) at speeds less than 45 m s^{-1} (87 kts) in Class E and G airspace below 914 m AGL and not exceeding ~~3657 m above mean sea level (MSL)~~ 3,657 m MSL in in the vicinity of Alamosa County, CO under the jurisdiction of the Denver Air Route Traffic Control Center (ARTCC). Typical COA provisions for airworthiness, operations, safety protocols, Notice to Airmen (NOTAMs), reporting, and registration were applied; however, special provisions were necessary for the coordination and deconfliction of the myriad of teams participating in flight operations as part of LAPSE-RATE. Instead of requiring each individual team to submit NOTAMs, discussions between LAPSE-RATE participants, the FAA, and Denver ARTCC lead to the definition of a common area of operations that could cover the entirety of the planned LAPSE-RATE observations. Additional deconfliction was also necessary with nearby airports, Military Training Routes (MTRs), or other restricted airspaces such as the Great Sand Dunes National Park. Within this area, two NOTAM subareas were defined so that the most appropriate areas could be activated with the necessary 24-hr notice based on the next day's scientific objectives. Emergency procedures for lost links, radio communications, and other potential anomalies also had special provisions due to the number of teams operating

Table 4. Summary of flights for each day broken down by aircraft and location. Local time during the campaign was Mountain Daylight Time (UTC−6).

Date	Time Start	Time Stop	Science Objective	Site 1	Aircraft Number	Flight Count	Site 2	Aircraft Number	Flight Count	Daily Total
14 July 2018	1430 UTC	2130 UTC	CASS Tests	MOFF	OU944	4	–	–	–	4
15 July 2018	1330 UTC	1945 UTC	CI	MOFF	OU944 OU955	2 18	K04V	OU946	14	34
16 July 2018	1330 UTC	2115 UTC	CI	MOFF	OU955	26	K04V	OU946	21	47
17 July 2018	1330 UTC	2130 UTC	CASS Tests	MOFF	OU944 ~~OU946~~	5 ~~9~~	~~–~~ MOFF	~~–~~OU946	~~–~~9	14
18 July 2018	1230 UTC	1945 UTC	ABL Transition	MOFF	OU944	14	K04V	OU946	21	35
19 July 2018	1115 UTC	1700 UTC	Drainage	MOFF	OU944	24	NSF	OU946	22	46
					MOFF Total	~~102~~ 93	**K04V & NSF Total**		~~78~~ 87	**180**

in proximity to each other. In addition to the COA provisions, each OU operations area was overseen by a licensed private pilot who assisted with overseeing the airspace and deconflicting RPAS operations from general aviation traffic.

CopterSonde missions were programmed to fly a vertical ascent from the surface to 914 m AGL, utilizing the platforms wind vane mode to continuously orient itself into the wind. This permitted the RPAS to sample the vertical structure of pressure, temperature, humidity, wind speed, and wind direction in a controlled and repeatable manner that minimized influences from the platform itself (Segales et al., 2020a). These flights will be referred to as profiles in subsequent text and tables. These profiles consisted of an automatic takeoff, vertical ascent at a rate of 3.5 m s^{-1}, loiter for 10 s at the apex of the ascent, and controlled decent to 10 m at a rate of 6 m s^{-1}. Once the platform completed its decent, it would be brought in for a landing manually. ~~To prevent dust and other debris from being sucked up into the scoop and possibly damaging the sensors when close to the ground, the ducted fan in the scoop was programmed to turn on at 1.85 m and off at 1.45 m AGL~~As will be discussed in Section 3, only the ascent portion of these vertical profiles are considered for analysis. We therefore chose to fly slower on the ascent to maximize the vertical resolution when accounting for thermodynamic sensor response times. Moreover, by descending more rapidly we are able to achieve a higher maximum profile altitude than we would otherwise with the same battery configuration on the CopterSonde.

Profiles were conducted on a 15- or 30-min cadence depending on the day's primary scientific objective and how rapidly the thermodynamic and kinematic parameters of the ABL were evolving. As the CopterSonde was collocated with CLAMPS at MOFF, RPAS profiles would often coincide with radiosonde launches. When this would occur, the RPAS launch would be held until the balloon cleared the airspace (about 60 s), and then would proceed as normal.

3 Data processing

The data collected by the CopterSondes were processed and quality controlled by CASS after the conclusion of the LAPSE-RATE campaign. The CopterSondes' Pixhawk autopilot system output and store a binary file on an on-board SD card during each flight, which includes logs of the aircraft's attitude angles, GPS positions, accelerations, and readings from the 3 temperature and 3 relative humidity sensors. In this format, the data are equivalent to the United States Department of Energy (DoE) Atmospheric Radiation Measurement (ARM) program's data archive "a0" level. Because the sensors log at different rates to the SD card, the binary files were converted to JavaScript Object Notation (JSON) format and relevant data parameters were interpolated/downsampled to a common 10 Hz time vector in comma-separated values (CSV) format (a1 level). The JSON file format allows for the varying sampling rates for each data stream to coexist in the same file, whereas the conversion to CSV with a common time vector markedly simplifies reading and processing the data at this stage. More information about how the CopterSonde fuses sensor readings with autopilot features can be found in Segales et al. (2020a), and the autopilot code is freely available at Segales et al. (2020b).

After converting the raw binary flight log files to csv format, offsets for each temperature and relative humidity sensor were applied. These offsets were determined in the manner described by Greene et al. (2019) and Segales et al. (2020a), which involved isolating the CopterSondes' front L-duct sensor payloads in an environmentally-controlled chamber operated by the Oklahoma Mesonet with National Institutes of Standards and Technology (NIST) traceable sensors as references. Furthermore, at this stage, the CopterSonde attitude angles were averaged to estimate the horizontal wind speed and direction using linear regression coefficients determined by hovering next to Oklahoma Mesonet towers as a reference. This process is outlined in Greene (2018) and Segales et al. (2020a) (based on Neumann and Bartholmai, 2015; Palomaki et al., 2017).

Once the thermodynamic and kinematic calibrations were accounted for, the post-processing algorithm objectively determined the window of time for evaluation. This was chosen to be between 6 m AGL and the maximum point of the direct vertical profile (typically 914 m AGL during LAPSE-RATE) on the *ascending* portion only, averaged to 3-m bins as estimated by the Pixhawk autopilot's barometer and GPS sensors (Segales et al., 2020a). These criteria were chosen for several reasons, primarily to do with the relationships between ascent rate and sensor response time. Data averaging began at 6 m so as to avoid any possible contamination due to propeller wash interacting with the ground. The ascent portion is chosen because the flight patterns of the CopterSonde were chosen to maximize the achievable flight altitude and involves descending much more rapidly than ascending. Therefore, the descent portion suffers more from thermodynamic sensor response time issues. Furthermore, the physics behind the method of estimating horizontal wind speeds are not the same given the body forcings on a descending rotary-wing RPAS. Finally, the 3 m averaging interval was chosen under consideration of the average ascent rate (3.5 m s^{-1}) and an approximate time constant of the sensor payload of 2 s. This time constant is based upon experiments during the ISOBAR18 campaign with an older version of the CopterSonde and identical sensors (Kral et al., 2020; Greene et al., 2021, in preparation), where the aircraft was subjected to a series of quasi-step-function inputs between a sauna and the below-freezing environment of Hailuoto, Finland. The averaging interval of 3 m is therefore approximately double the vertical resolution as predicted by the response time and ascent rate, so further studies will be needed to elucidate the impacts of these decisions.

Because the CopterSondes were outfitted with 3 temperature and 3 RH sensors each, it was necessary to inspect each of their time-series outputs with respect to one another to determine potential outliers. Although an objective method of doing so is ideal, research into this is still ongoing and thus we chose to subjectively analyze each sensor individually. A given sensor was omitted from further consideration if it did not correlate with the other sensors and/or there was a large bias between them (greater than 0.5°C). All remaining sensor data were averaged together to yield a single measurement of temperature and relative humidity at each 3-m altitude interval. With an average ascent rate of 3.5 m s^{-1} and a 10 Hz sampling rate, this corresponds to 8–9 samples per sensor per altitude averaging bin. These post-processed ascent profiles were then exported in netCDF format (b1 level) that contain self-describing metadata including e.g., the specific aircraft and flight description. These file contents are described in Table 2.

In an effort to quantify the CopterSonde thermodynamic and kinematic observational biases relative to a ubiquitous standard, Bell et al. (2020a) compared vertical profile CopterSonde flights from LAPSE-RATE and in Oklahoma to collocated Vaisala RS92-SGP radiosondes. While unable to explicitly account for factors such as horizontal heterogeneity, the sample ranges in temperature, dewpoint temperature, and horizontal winds were large enough to determine baseline accuracies in each (Table 2). Namely, CopterSonde temperatures were within 0.5°C of the radiosondes in the aggregate, which is largely due in part to the considerations taken for temperature sensor placement on-board the CopterSonde (Greene et al., 2018, 2019). Additionally, a broad intercomparison effort during the LAPSE-RATE campaign (Barbieri et al., 2019) resulted in similar statistics when comparing the CopterSonde observations to a common mobile meteorological reference.

4 Examples of Flight Data

4.1 Convective Initiation – 15 July 2018

The environment on the morning of 15 July 2018 was rich in moisture with decreasing stability as the day progressed. This made ~~it a good day~~ for good conditions to target pre-convective measurements. The low wind shear and weak synoptic flow were conducive for isolated CI. This aided in spatially discerning precursors to CI. Two CASS teams were stationed at ~~MOFF and~~ K04V and MOFF, approximately 18 km apart, with aircraft OU946 and OU955, respectively. Both teams began flying at 1400 UTC (0900 MDT). The team at ~~MOFF conducted profiles every 15 minutes until 1945 UTC (1445~~ K04V flew profiles every 30 minutes until 1830 UTC (1330 MDT). The team at ~~K04V conducted profiles nearly every 30 minutes until 1915 UTC (1415~~ MOFF had profiles every 15 minutes until 1945 UTC (1445 MDT). The cadence was reduced to 30 minutes once the ABL had become mixed at 1500 UTC (1000 MDT). At 1830 UTC (1330 MDT), there was convection in the vicinity and flight cadence was increased to 15 minutes at both sites. The maximum flight height for both teams was 914 m~~AGL~~.

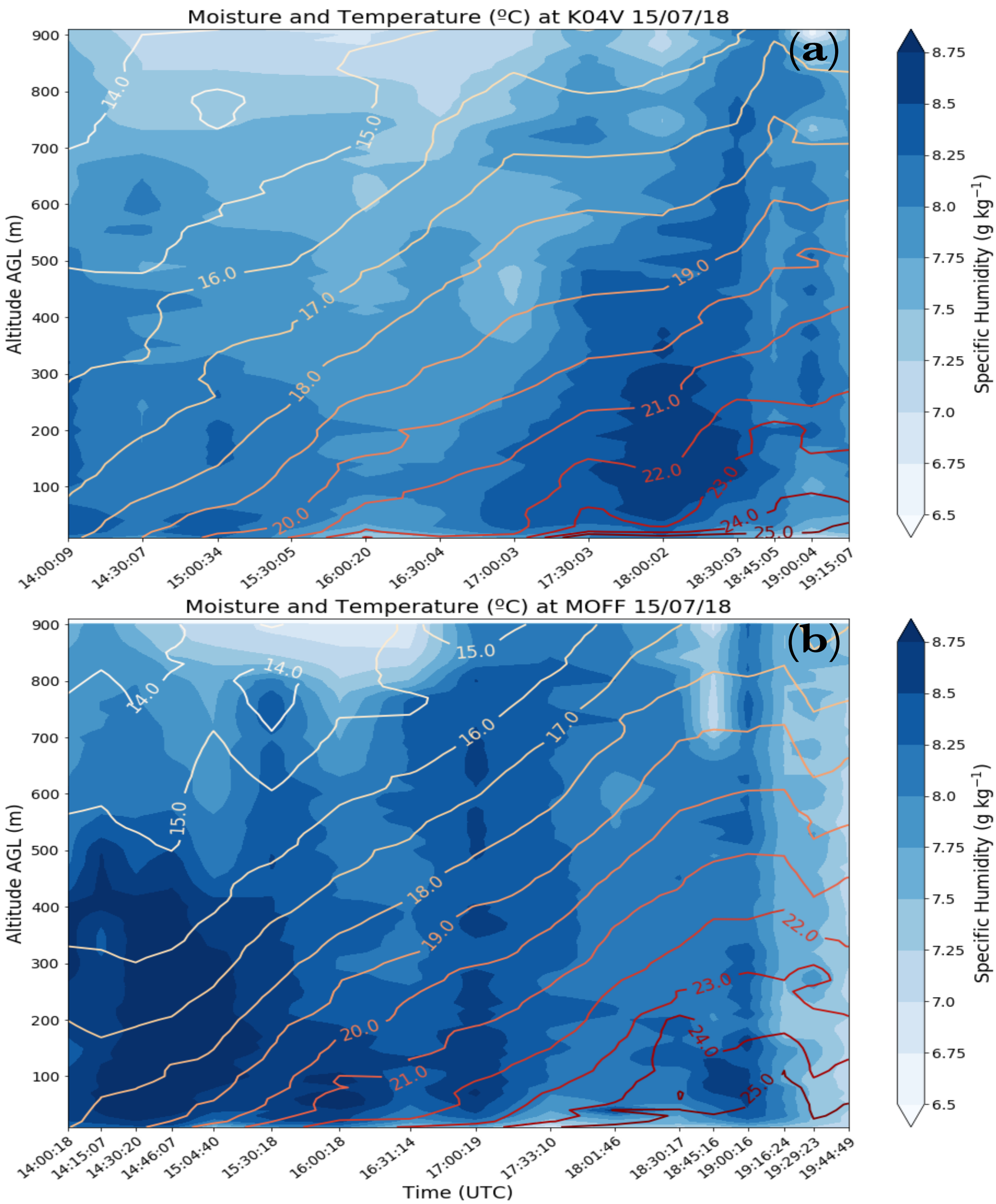

Figure 3. Time-height cross-section view of moisture and ~~buoyancy~~ temperature measurements ~~at K04V on~~ 15 July 2018. a) K04V site. b) MOFF site. This day experienced deep convection. Each time tick indicates a flight. Shaded field is specific humidity (g kg^{-1}). Contours are ~~buoyancy where blue~~ temperature (~~negative~~°C)~~and red (positive) (m s^{-2})~~. Values are interpolated through time at each level between successive flights.

Figures ~~?? and ??~~ 3a and 3b show differences in how moisture and ~~low-level buoyancy~~ temperature evolve with time at each site. Figure~~??~~ 3a shows specific humidity increasing at K04V with time, meanwhile decreasing at MOFF (Figure ~~??). Low-level buoyancy poses a different way to evaluate pre-convective environments. Buoyancy was calculated by taking the temperature difference of the environment (observed) and a parcel lifted adiabatically from the surface calculated from the observed surface temperature . Figure **??** showed that there is a strong buoyancy gradient in time from 1700 – 1730 UTC. Around 1730 UTC, deep CI formed nearby~~ 3b). Evaporation of additional moisture over MOFF slowed daytime heating. Although both sites had similar temperature fields, Figure 3a shows the temperature increasing faster with time. Since K04V ~~. However, more cases~~ was slightly drier, this led to faster destabilization and possibly preferential CI. Figure 3a also shows cooler temperatures below 300 m at 1800 UTC. At 100 m, K04V is 2 °C cooler than at MOFF. This may have been caused by outflow from a nearby storm. Even though the sites were not very far apart, there is a difference in the evolution of specific humidity. More cases would need to be ~~studied~~ analyzed to determine if this ~~is a common observance before~~ could have implicated the location of CI. Further analysis of the evolution of low-level buoyancy preceding this case is conducted in Lappin and Chilson (2021, in preparation). Previously, buoyancy has been used as a bulk stability parameter to determine storm severity (Zhang and Klein, 2010; Trier et al., 2014). This study looks into using buoyancy as a prognostic variable sensitive in time and space. It aims to discern local differences in ABL evolution in convective environments and further understanding of CI.

~~Time-height cross-section view of moisture and buoyancy measurements at MOFF on 15 July 2018. This day experienced deep convection. Shaded field is specific humidity (g kg^{-1}). Contours are buoyancy where blue (negative) and red (positive) (m s^{-2}). Values are interpolated through time at each level between successive flights.~~

4.2 CASS Test Flights – 17 July 2018

The LAPSE-RATE participants collectively decided for 17 July 2018 ~~was collectively decided by the LAPSE-RATE participants~~ to be utilized for individual group research objectives, and so both mobile CASS teams decided to combine at the MOFF site for intercomparison flights between the CopterSondes and against CLAMPS. Between OU944 and OU946, 14 total vertical profile flights were conducted throughout the afternoon, 8 of which were simultaneous for direct comparisons across platforms (Table 4). Several of these flights were also accompanied by radiosonde launches directly before the vertical profiles, which were included along with the CLAMPS AERI and Doppler LIDAR observations in the comparison study by Bell et al. (2020a). The LAPSE-RATE ground-based remote sensing data is outlined by Bell et al. (2020b). During these flights, the pair of CopterSondes flew about 10–20 m apart horizontally, and were also displaced about 50 m from the radiosonde launch site. An example of a direct comparison between OU944 and OU946 on the afternoon of ~~the~~ 17 ~~th~~ July (Figure 4) shows that both aircraft observed similar thermodynamic features with a well-mixed, dry adiabatic atmosphere up to around 600 m AGL, above which is notably drier and warmer than the ABL below. ~~While a small bias~~ Although the general profile shapes and inversion magnitudes are consistent across the platforms, a bias in temperature is apparent especially in the lowest 100 m. These discrepancies in the temperatures between the two ~~aircraft exists in temperature andspecific humidity, the profile shapes and inversion magnitudes are consistent across the platforms. Furthermore,~~ identical platforms can likely be attributed to three

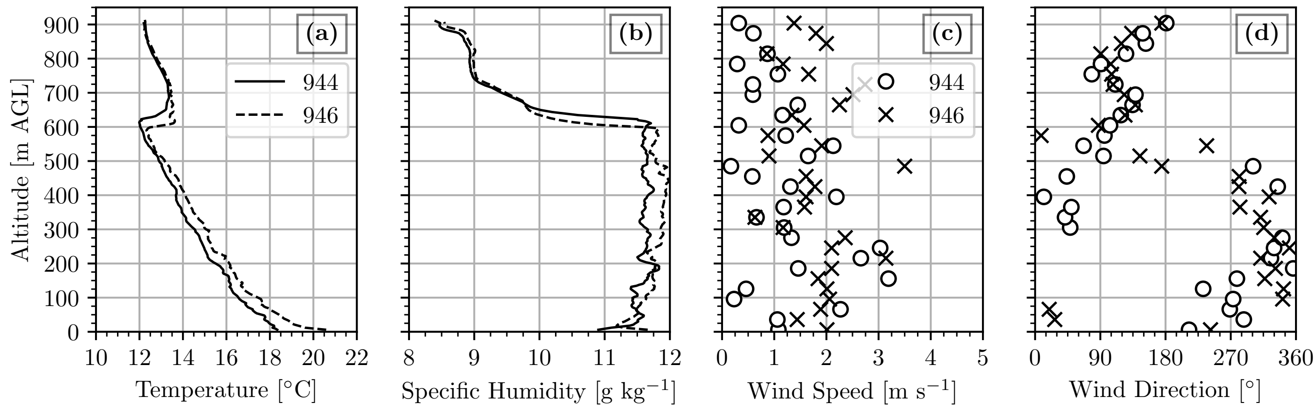

Figure 4. Comparisons of two CopterSonde flights launched simultaneously at 16:02:55 UTC at MOFF on 17 July 2018. ~~In all panels, the solid and dashed black lines represent the OU944 and OU946 aircraft, respectively.~~ Shown here are (a) temperature (°C), (b) specific humidity (g kg^{-1}), ~~and~~ (c) horizontal wind speed (m s^{-1}), and (d) horizontal wind direction (degrees) versus altitude above ground level (AGL). Note that all data are included in (a) and (b), but data are subsampled at every eight points in (c) and (d) for clarity. In (a) and (b) ((c) and (d)), the solid and dashed black lines (open circles and Xs) represent the OU944 and OU946 aircraft, respectively. Wind speed and direction in general throughout the campaign were considerably variable in time and space.

main sources: 1) sunlight on an inadequately shielded sensor (discussed in Greene et al., 2019) at the correct relative angles of aircraft heading and sun zenith/azimuth; 2) natural variability in the atmosphere: the two aircraft were 10—20 m apart, so this is not entirely unreasonable for a convective boundary layer; and/or 3) systemic bias related to calibration of the CopterSonde thermodynamic sensor package as a whole. While a combination of these three is the most likely explanation, we believe the spatial/temporal heterogeneity of the atmosphere during these observations should not be overlooked. For example, 3 s sonic anemometer temperatures from Bailey et al. (2020) reveal that during the 10 min timeframe during these concurrent CopterSonde profiles (albeit at a different site but featuring similar land cover properties), 2 m temperatures fluctuated by up to 4°C. Doppler lidar observed vertical velocities collocated with the CopterSondes (Bell et al., 2020a, b) also indicate roughly 3 m s^{-1} updrafts at the same time as the profiles in Figure 4. Turbulent transport of temperature therefore likely contributed to large spatial and temporal heterogeneity that can be detectable at the 10–20 m separation scales in this particular comparison flight.

Moreover, the horizontal winds throughout the depth of the atmosphere were weak and variable ~~, but still show reasonable agreement between the two aircraft.~~ during these profiles, but observations from both aircraft demonstrate reasonable agreement (Figure 4c). As discussed previously, the CopterSonde estimates horizontal wind speeds and directions based on a second-order least-squares regression fit between the aircraft's tilt angle into the wind (calculated from three-dimensional Euler rotation matrices) and an Oklahoma Mesonet 10 m wind reference (Greene, 2018; Segales et al., 2020a). As more sophisticated autopilot-based adaptive wind estimation techniques become available, future studies should leverage this particular dataset along with other ground-based sensors (Bell et al., 2020b) or large eddy simulations (Pinto et al., 2020) to examine the effects of spatial and

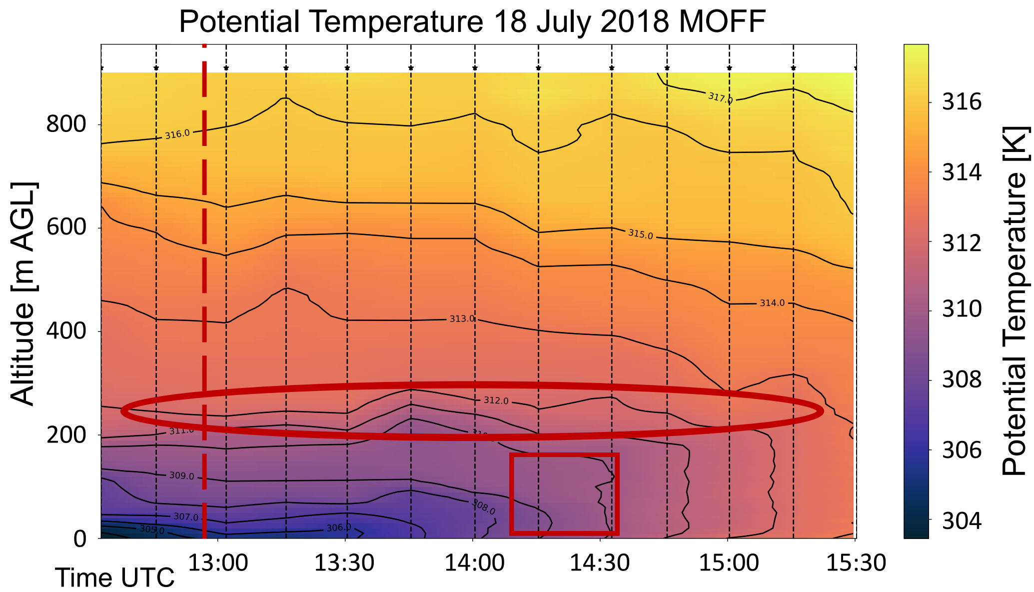

Figure 5. Time-height cross-section view of CopterSonde potential temperature observations at the MOFF on 18 July 2018. Shaded and contoured are potential temperature (K), and vertical dashed lines represent the time of CopterSonde flights. The star markers represent the maximum altitude achieved for a given profile. Values are interpolated through time at each level between successive flights. See text for discussion on the features annotated in red.

temporal heterogeneity on instruments located less than 100 m apart. For a more detailed perspective on the relative accuracy and precision of this dataset, readers are again referred to Barbieri et al. (2019) and Bell et al. (2020a).

4.3 Boundary Layer Transition – 18 July 2018

The morning of 18 July 2018, featured weak ambient synoptic-scale weather conditions and clear skies throughout the valley that enabled targeted measurements of the diurnal ABL transition. On this day, the two CASS teams were situated at the ~~MOFF and~~ K04V and MOFF sites, with operations taking place from 1230–1945 UTC (0630–1345 MDT; Table 4). At both locations, vertical profiles to 914 m AGL were flown once every 15 min for the majority of the day. This particular case exemplified a canonical morning ABL transition, marked by a surface-based temperature inversion with a residual layer apparent atop beginning around 300 m at local sunrise, which occurred at 5:55 AM MDT (Figure 5, vertical red dashed line). After the sun rose above the Rocky Mountains and flooded the valley with shortwave radiation, vertical mixing dominated the lowest levels of the ABL. A surface-based dry adiabatic layer became present around 1415 UTC (Figure 5, red rectangle) as the ABL grew in depth. Surface-based vertical mixing appears to dominate the surface layer for several hours this morning, as the atmosphere above 300 m remains relatively steady-state for most of the early growth of the convective boundary layer. Entrainment-based

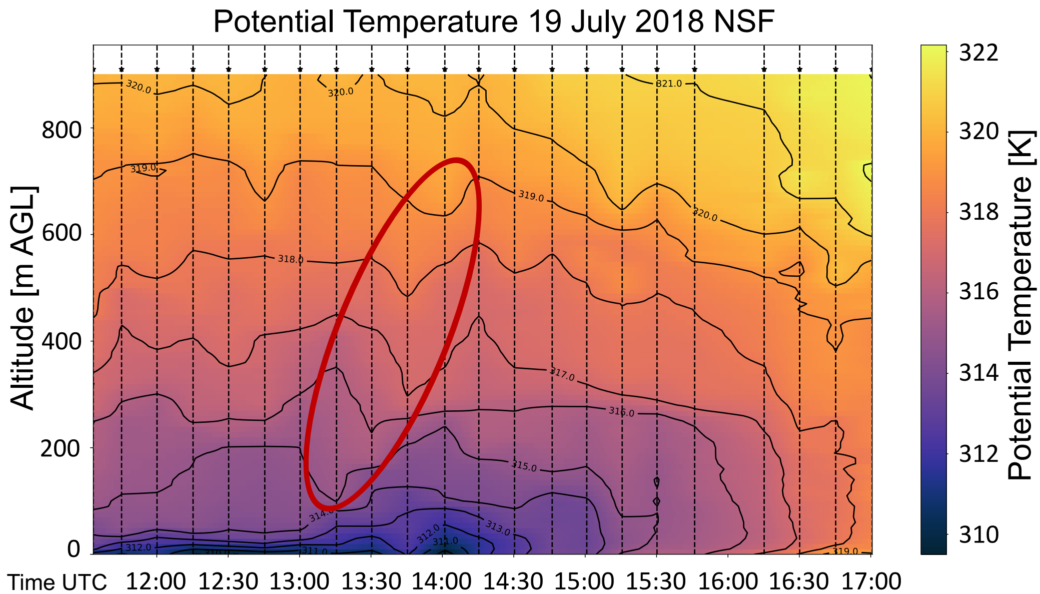

Figure 6. Time-height cross-section view of CopterSonde potential temperature observations at the ~~Saguache farm~~ North Star Farm (NSF) location on 19 July 2018. Figure notations follow the same conventions as in Figure 5. See text for discussion on the features annotated in red.

heating of the growing ABL is also apparent by tracking the level of the strongest vertical potential temperature gradient through the morning (Figure 5, red oval).

4.4 Drainage Flow – 19 July 2018

The morning of 19 July 2018, was characterized by relatively quiescent conditions, making it the target of katabatic drainage flow observations. CASS flew CopterSondes from two locations (MOFF and NSF), conducting 46 total vertical profiles at 15 min intervals between 1115–1700 UTC (Table 4). A cursory glance at potential temperature in time-height coordinates from this day at the NSF site (Figure 6) reveals a similar ABL transition as observed on the previous day from the MOFF site (Figure 5). Wind speed and direction (Figure 7a, b) are also weak but primarily from the east below 400 m and from the north above 500 m. However, closer inspection reveals several harmonic structures, with a relative warm anomaly around 100 m AGL with a period of roughly 15 min at 1315 UTC propagating vertically through the next 4–5 profiles (Figure 6, red oval). Due to the highly stratified nature of the atmosphere at this time and the presence of complex topography, it is possible these disturbances are the result of internal gravity waves. Further investigation is necessary to elucidate specific details on this phenomenon and its sensitivity to spatial and temporal interpolation schemes.

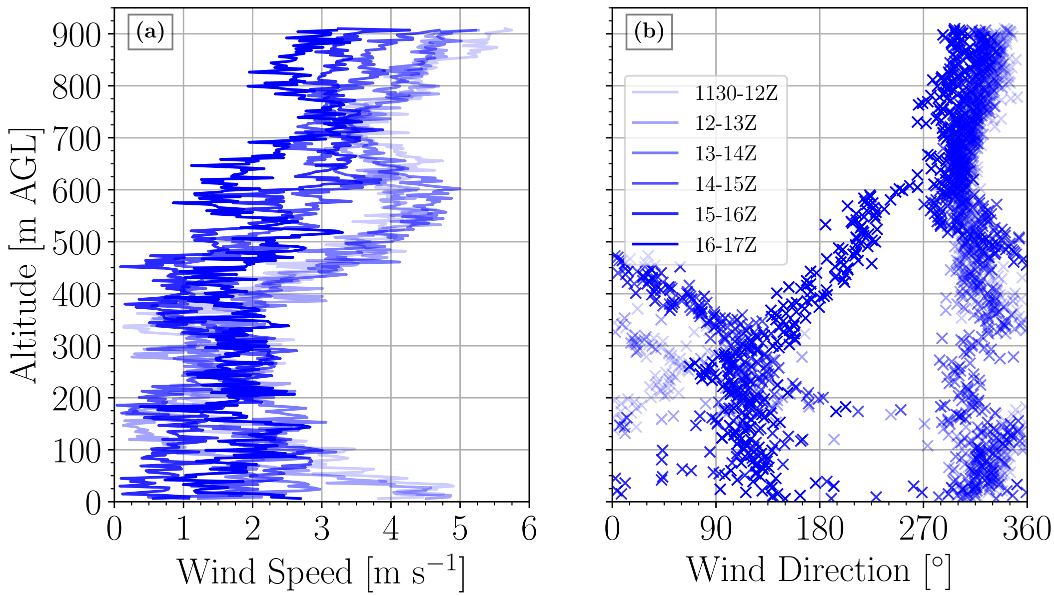

Figure 7. Hourly average profiles of wind speed (a) and wind direction (b) at the North Star Farm locations 19 July 2018.

5 ~~Data processing~~

~~The data collected by the CopterSondes were processed and quality controlled by CASS after the conclusion of the LAPSE-RATE campaign. The CopterSondes' Pixhawk autopilot system output and store a binary file on an on-board SD card during each flight, which includes logs of the aircraft's attitude angles, GPS positions, accelerations, and readings from the 3 temperature and 3 relative humidity sensors. In this format, the data are equivalent to the United States Department of Energy (DoE) Atmospheric Radiation Measurement (ARM) program's data archive "a0" level. Because the sensors log at different rates to the SD card, the binary files were converted to JavaScript Object Notation (JSON) format and relevant data parameters were interpolated/downsampled to a common 10 Hz time vector in comma-separated values (CSV) format (a1 level).~~

~~After converting the raw binary flight log files to csv format, offsets for each temperature and relative humidity sensor were applied. These offsets were determined in the manner described by Greene et al. (2019) and Segales et al. (2020a), which involved isolating the CopterSondes' front L-duct sensor payloads in an environmentally-controlled chamber operated by the Oklahoma Mesonet with National Institutes of Standards and Technology (NIST) traceable sensors as references. Furthermore, at this stage, the CopterSonde attitude angles were averaged to estimate the horizontal wind speed and direction using linear regression coefficients determined by hovering next to Oklahoma Mesonet towers as a reference. This process is outlined in Greene (2018) and Segales et al. (2020a) (based on Neumann and Bartholmai, 2015; Palomaki et al., 2017).~~

~~Once the thermodynamic and kinematic calibrations were accounted for, the post-processing algorithm objectively determined the window of time for evaluation. This was chosen to be between 6 m AGL and the maximum point of the direct vertical~~

~~profile (typically 914 m AGL during LAPSE-RATE) on the *ascending* portion only, averaged to 3-m bins as estimated by the Pixhawk autopilot's barometer and GPS sensors (Segales et al., 2020a). These criteria were chosen for several reasons, primarily to do with the relationships between ascent rate and sensor response time. Data averaging began at 6 m so as to avoid any possible contamination due to propeller wash interacting with the ground. The ascent portion is chosen because the flight patterns of the CopterSonde were chosen to maximize the achievable flight altitude and involves descending much more rapidly than ascending. Therefore, the descent portion suffers more from thermodynamic sensor response time issues. Furthermore, the physics behind the method of estimating horizontal wind speeds are not the same given the body forcings on a descending rotary-wing RPAS. Finally, the 3 m averaging interval was chosen as a combination of ascending at 3 m s^{-1} and an approximate time constant of the sensor payload of 1 s.~~

~~In this window of time for analysis, time-series data from each of the temperature and relative humidity sensors were plotted and relative outlier sensors were subjectively omitted from further processing if they did not qualitatively or quantitatively follow the trends of the other sensors. All remaining sensor data were averaged together to yield a single measurement of temperature and relative humidity at each 3-m altitude interval. These post-processed ascent profiles were then exported in netCDF format (b1 level) that contain self-describing metadata including e.g., the specific aircraft and flight description. These file contents are described in Table 2. The reader is directed to Barbieri et al. (2019) and Bell et al. (2020a) for more information on measurement accuracy, and Greene et al. (2018, 2019) for more regarding considerations taken for temperature sensor placement on-board the CopterSonde.~~

~~Description of the thermodynamic and kinematic parameters available in each CopterSonde data file. Also includes information on the method each parameter was measured along with their relative accuracies based on Bell et al. (2020a) compared to Vaisala RS92-SGP radiosondes.~~ ~~**Parameter Method Accuracy**~~ ~~Temperature 3 iMet-XF Bead Thermistors ±0.5°C Relative Humidity 3 IST HYT-271 Capacative HygrometersConverted to dewpoint temperature then recalculatedusing fast-response iMet-XF bead thermistors±2% Dewpoint Temperature Converted from temperature and relative humiditymeasured by the 3 IST HYT-271 sensors±0.5°C Pressure TE MS5611 Barometric Pressure Sensor (inside Pixhawk 2.1 Autopilot) ±1.5 hPa Wind Speed Linear regression of tilt anglescompared to reference±0.6 m s^{-1} Wind Direction Linear regression of tilt anglescompared to reference±4°~~

5 Data availability

The OU CopterSonde data files from the LAPSE-RATE campaign are available for public access from the Zenodo data repository ~~(Greene et al., 2020)~~(Greene et al., 2020, DOI:10.5281/zenodo.3737087). They are in netCDF format with self-describing metadata and are organized by flight, aircraft tail number, and location. Included in each file are quality-controlled thermodynamic (temperature, pressure, humidity) and kinematic (wind speed and direction) measurements from collected by CASS during the LAPSE-RATE campaign from 14–19 July 2018. These files are from the fleet of 3 individual CopterSonde rotary-wing RPAS used during the campaign.

The files follow a naming convention of UOK.ppppp.lv.yyyymmdd.hhmmss.cdf, where ppppp is a platform identification code (one of "OU944", "OU946", "OU955"), lv is the data file processing level, and yyyymmdd.hhmmss is the year-month-date.hour-minute-second of the file start date and time. Further information is included in the readme text file in this repository.

6 Summary

During July 2018, researchers from OU's ~~Center for Atmospheric Sampling and Sensing (CASS)~~ CASS participated alongside federal and university partners in the LAPSE-RATE field campaign in San Luis Valley, Colorado, USA. The OU team successfully completed 180 flights using three RPAS over the course of six days of operation to collect vertical profiles of the thermodynamic and kinematic state of the ABL. This article describes sampling strategies, data collection, platform ~~intercomparibility~~intercomparability, data quality and processing, and the dataset's possible applications to convective initiation, drainage flows, and ABL transitions.

The data available from these flights provides measurements of temperature, humidity, pressure, wind speed, and wind direction at a higher ~~spatiotempral~~ spatiotemporal resolution in the ABL ~~then~~ than many conventional strategies, such as radiosondes, which will significantly contribute to characterizing the ABL within the San Luis Valley during the campaign. The data collected from the operations and platforms described here are uploaded and available for download through the Zenodo data repository (~~link goes here).~~ DOI:10.5281/zenodo.3737087). This data has already been featured in studies comparing RPAS profiling accuracies to those from more traditional profilers such as radiosondes, LIDARs, and AERIs (Bell et al., 2020a; Segales et al., 202 . It will also be utilized in several ongoing studies that examine the use of RPAS data to improve temperature forecasts impacted by valley drainage flows (de Boer et al., 2020a) and the utility of using buoyancy as a metric to understand convection initiation and boundary layer transitions (Lappin and Chilson, 2021, in preparation).

Author contributions. Field Campaign Planning: E.P.L and P.C.; Data Collection: E.P.L, B.G., T.B., A.S., G.A., W.D, S.K., D.T., and P.C.; Data processing and quality control: B.G.; Data Analysis and Visualization: B.G., F.L., and T.B.; Writing: E.P.L, B.G., and F.L.; Supervision: P.C. and E.P.L; Funding acquisition: P.C.

Competing interests. The authors declare that they have no conflicts of interest.

Acknowledgements. This research has been supported in part by the National Science Foundation under Grant No. 1539070 and internal funding from the University of Oklahoma Office of the Vice President for Research and Partnerships. The authors would also like to thank the Moffat Consolidated School for the use of their parking lot and facilities for the duration of the campaign as well as the greater San Luis Valley community for welcoming the LAPSE-RATE campaign and providing land access for flight operations. Additional support for field operations in Colorado were provided by University of Oklahoma undergraduate research assistants Brandon Albert, Samantha Bashcky, Christopher Hughes, Mark Thiel, and Brent Wolf.

References

Bailey, S. C. C., Sama, M. P., Canter, C. A., Pampolini, L. F., Lippay, Z. S., Schuyler, T. J., Hamilton, J. D., MacPhee, S. B., Rowe, I. S., Sanders, C. D., Smith, V. G., Vezzi, C. N., Wight, H. M., Hoagg, J. B., Guzman, M. I., and Smith, S. W.: University of Kentucky measurements of wind, temperature, pressure and humidity in support of LAPSE-RATE using multisite fixed-wing and rotorcraft unmanned aerial systems, Earth System Science Data, 12, 1759–1773, https://doi.org/10.5194/essd-12-1759-2020, 2020.

Barbieri, L., Kral, S. T., Bailey, S. C., Frazier, A. E., Jacob, J. D., Reuder, J., Brus, D., Chilson, P. B., Crick, C., Detweiler, C., et al.: Intercomparison of small unmanned aircraft system (sUAS) measurements for atmospheric science during the LAPSE-RATE campaign, Sensors, 19, 2179, https://doi.org/https://doi.org/10.3390/s19092179, 2019.

Bell, T. M., Greene, B. R., Klein, P. M., Carney, M., and Chilson, P. B.: Confronting the boundary layer data gap: evaluating new and existing methodologies of probing the lower atmosphere, Atmospheric Measurement Techniques, 13, 3855–3872, https://doi.org/10.5194/amt-13-3855-2020, 2020a.

Bell, T. M., Klein, P. M., Lundquist, J. K., and Waugh, S.: Remote sensing and radiosonde datasets collected in the San Luis Valley during the LAPSE-RATE campaign, Earth System Science Data Discussions, 2020, 1–19, https://doi.org/10.5194/essd-2020-314, 2020b.

Bonin, T., Chilson, P., Zielke, B., and Fedorovich, E.: Observations of the Early Evening Boundary-Layer Transition Using a Small Unmanned Aerial System, Boundary-Layer Meteorology, 146, 119–132, https://doi.org/10.1007/s10546-012-9760-3, 2012.

Bonin, T., Chilson, P., Zielke, B., Klein, P., and Leeman, J.: Comparison and application of wind retrieval algorithms for small unmanned aerial systems, Geoscientific Instrumentation, Methods and Data Systems, 2, 177–187, https://doi.org/10.5194/gi-2-177-2013, 2013.

Bonin, T. A., Blumberg, W. G., Klein, P. M., and Chilson, P. B.: Thermodynamic and turbulence characteristics of the southern great plains nocturnal boundary layer under differing turbulent regimes, Boundary-Layer Meteorology, 157, 401–420, https://doi.org/10.1007/s10546-015-0072-2, 2015.

Brosy, C., Krampf, K., Zeeman, M., Wolf, B., Junkermann, W., Schäfer, K., Emeis, S., and Kunstmann, H.: Simultaneous multicopter-based air sampling and sensing of meteorological variables, Atmospheric Measurement Techniques, 10, 2773–2784, https://doi.org/10.5194/amt-10-2773-2017, 2017.

Brus, D., Gustafsson, J., Kempinen, O., de Boer, G., and Hirsikko, A.: Atmospheric aerosol, gases and meteorological parameters measured during the LAPSE-RATE campaign, Earth System Science Data Discussions, 2020, 1–19, https://doi.org/10.5194/essd-2020-251, 2020.

Chilson, P. B., Bell, T. M., Brewster, K. A., Britto Hupsel de Azevedo, G., Carr, F. H., Carson, K., Doyle, W., Fiebrich, C. A., Greene, B. R., Grimsley, J. L., et al.: Moving towards a Network of Autonomous UAS Atmospheric Profiling Stations for Observations in the Earth's Lower Atmosphere: The 3D Mesonet Concept, Sensors, 19, 2720, https://doi.org/https://doi.org/10.3390/s19122720, 2019.

de Boer, G., Argrow, B., Cassano, J., Cione, J., Frew, E., Lawrence, D., Wick, G., and Wolff, C.: Advancing Unmanned Aerial Capabilities for Atmospheric Research, Bulletin of the American Meteorological Society, 100, ES105–ES108, https://doi.org/10.1175/BAMS-D-18-0254.1, 2019.

de Boer, G., Diehl, C., Jacob, J., Houston, A., Smith, S. W., Chilson, P., Schmale, David G., I., Intrieri, J., Pinto, J., Elston, J., Brus, D., Kemppinen, O., Clark, A., Lawrence, D., Bailey, S. C. C., Sama, M. P., Frazier, A., Crick, C., Natalie, V., Pillar-Little, E., Klein, P., Waugh, S., Lundquist, J. K., Barbieri, L., Kral, S. T., Jensen, A. A., Dixon, C., Borenstein, S., Hesselius, D., Human, K., Hall, P., Argrow, B., Thornberry, T., Wright, R., and Kelly, J. T.: Development of Community, Capabilities, and Understanding through Unmanned Aircraft-Based Atmospheric Research: The LAPSE-RATE Campaign, Bulletin of the American Meteorological Society, 101, E684–E699, https://doi.org/10.1175/BAMS-D-19-0050.1, 2020a.

de Boer, G., Houston, A., Jacob, J., Chilson, P. B., Smith, S. W., Argrow, B., Lawrence, D., Elston, J., Brus, D., Kemppinen, O., Klein, P., Lundquist, J. K., Waugh, S., Bailey, S. C. C., Frazier, A., Sama, M. P., Crick, C., Schmale III, D., Pinto, J., Pillar-Little, E. A., Natalie, V., and Jensen, A.: Data Generated During the 2018 LAPSE, Earth System Science Data Discussions, 2020, 1–15, https://doi.org/10.5194/essd-2020-98, 2020b.

de Boer, G., Waugh, S., Erwin, A., Borenstein, S., Dixon, C., Shanti, W., Houston, A., and Argrow, B.: Measurements from mobile surface vehicles during LAPSE-RATE, Earth System Science Data Discussions, 2020, 1–28, https://doi.org/10.5194/essd-2020-173, 2020c.

Elston, J., Argrow, B., Stachura, M., Weibel, D., Lawrence, D., and Pope, D.: Overview of Small Fixed-Wing Unmanned Aircraft for Meteorological Sampling, Journal of Atmospheric and Oceanic Technology, 32, 97–115, https://doi.org/10.1175/JTECH-D-13-00236.1, 2015.

Glasheen, K., Pinto, J., Steiner, M., and Frew, E.: Assessment of Finescale Local Wind Forecasts Using Small Unmanned Aircraft Systems, Journal of Aerospace Information Systems, 17, 182–192, https://doi.org/10.2514/1.I010747, 2020.

Greene, B. R.: Boundary Layer Profiling Using Rotary-Wing Unmanned Aircraft Systems: Filling the Atmospheric Data Gap, Master's thesis, The University of Oklahoma, https://hdl.handle.net/11244/301374, 2018.

Greene, B. R., Segales, A. R., Waugh, S., Duthoit, S., and Chilson, P. B.: Considerations for temperature sensor placement on rotary-wing unmanned aircraft systems, Atmospheric Measurement Techniques, 11, 5519–5530, https://doi.org/10.5194/amt-11-5519-2018, 2018.

Greene, B. R., Segales, A. R., Bell, T. M., Pillar-Little, E. A., and Chilson, P. B.: Environmental and sensor integration influences on temperature measurements by rotary-wing unmanned aircraft systems, Sensors, 19, 1470, 2019.

Greene, B. R., Bell, T. M., Pillar-Little, E. A., Segales, A. R., Britto Hupsel de Azevedo, G., Doyle, W., Tripp, D. D., Kanneganti, S. T., and Chilson, P. B.: University of Oklahoma CopterSonde Files from LAPSE-RATE, https://doi.org/10.5281/zenodo.3737087, 2020.

Greene, B. R., Kral, S. T., Chilson, P. B., and Reuder, J.: Gradient-based turbulence estimates from multicopter profiles of the stable boundary layer during ISOBAR18, Boundary-Layer Meteorology, 2021, in preparation.

Jacob, J., Chilson, P., Houston, A., and Smith, S.: Considerations for atmospheric measurements with small unmanned Aircraft systems, Atmosphere, 9, 252, https://doi.org/https://doi.org/10.3390/atmos9070252, 2018.

Koch, S. E., Fengler, M., Chilson, P. B., Elmore, K. L., Argrow, B., Andra, D. L., and Lindley, T.: On the Use of Unmanned Aircraft for Sampling Mesoscale Phenomena in the Preconvective Boundary Layer, Journal of Atmospheric and Oceanic Technology, 35, 2265–2288, https://doi.org/10.1175/JTECH-D-18-0101.1, 2018.

Kral, S. T., Reuder, J., Vihma, T., Suomi, I., Haualand, K. F., Urbancic, G. H., Greene, B. R., Steeneveld, G.-J., Lorenz, T., Maronga, B., Jonassen, M. O., Ajosenpää, H., Båserud, L., Chilson, P. B., Holtslag, A. A. M., Jenkins, A. D., Kouznetsov, R., Mayer, S., Pillar-Little, E. A., Rautenberg, A., Schwenkel, J., Seidl, A. W., and Wrenger, B.: The Innovative Strategies for Observations in the Arctic Atmospheric Boundary Layer Project (ISOBAR): Unique fine-scale observations under stable and very stable conditions, Bull. Amer. Meteor. Soc., pp. 1 – 64, https://doi.org/10.1175/BAMS-D-19-0212.1, 2020.

Lappin, F. M. and Chilson, P. B.: Low-level buoyancy as a tool to understand boundary layer transitions, Atmospheric Measurements Techniques, 2021, in preparation.

Lee, T. R., Buban, M., Dumas, E., and Baker, C. B.: A New Technique to Estimate Sensible Heat Fluxes around Micrometeorological Towers Using Small Unmanned Aircraft Systems, Journal of Atmospheric and Oceanic Technology, 34, 2103–2112, https://doi.org/10.1175/JTECH-D-17-0065.1, 2017.

Lee, T. R., Buban, M., Dumas, E., and Baker, C. B.: On the Use of Rotary-Wing Aircraft to Sample Near-Surface Thermodynamic Fields: Results from Recent Field Campaigns, Sensors, 19, https://doi.org/10.3390/s19010010, 2018.

Neumann, P. P. and Bartholmai, M.: Real-time wind estimation on a micro unmanned aerial vehicle using its inertial measurement unit, Sensors and Actuators A: Physical, 235, 300–310, https://doi.org/10.1016/j.sna.2015.09.036, 2015.

Palomaki, R. T., Rose, N. T., van den Bossche, M., Sherman, T. J., and De Wekker, S. F.: Wind estimation in the lower atmosphere using multirotor aircraft, Journal of Atmospheric and Oceanic Technology, 34, 1183–1191, https://doi.org/10.1175/JTECH-D-16-0177.1, 2017.

Pinto, J. O., Jensen, A. A., Jiménez, P. A., Hertneky, T., Muñoz Esparza, D., Dumont, A., and Steiner, M.: Realtime WRF LES Simulations to Support UAS Flight Planning and Operations During 2018 LAPSE-RATE, Earth System Science Data Discussions, 2020, 1–36, https://doi.org/10.5194/essd-2020-242, 2020.

Segales, A. R., Greene, B. R., Bell, T. M., Doyle, W., Martin, J. J., Pillar-Little, E. A., and Chilson, P. B.: The CopterSonde: an insight into the development of a smart unmanned aircraft system for atmospheric boundary layer research, Atmospheric Measurement Techniques, 13, 2833–2848, https://doi.org/10.5194/amt-13-2833-2020, 2020a.

Segales, A. R., Tridgell, A., Mackay, R., Barker, P., Marchi, L. D., WickedShell, Riseborough, P., Pittenger, T., jason4short, Kancir, P., jschall, Hall, L., de Sousa, G. J., Oborne, M., Walser, J., Hickey, P., Lucas, A., Lefebvre, R., Purohit, S. B., Ferreira, F., murata, k., de Oliveira Filho, C. M., Staroselskii, G., Morphett, G., Denecke, M., Whitehorn, M., Hall, P., Shamaev, E., Jehangir, R., Goppert, J., and Vilches, V. M.: oucass/CASS-ardupilot: CASSv1.6.0-Copter-3.6.12, https://doi.org/10.5281/zenodo.3494655, 2020b.

Trier, S. B., Davis, C. A., Ahijevych, D. A., and Manning, K. W.: Use of the parcel buoyancy minimum (B min) to diagnose simulated thermodynamic destabilization. Part I: Methodology and case studies of MCS initiation environments, Monthly Weather Review, 142, 945–966, 2014.

Wagner, T. J., Klein, P. M., and Turner, D. D.: A New Generation of Ground-Based Mobile Platforms for Active and Passive Profiling of the Boundary Layer, Bulletin of the American Meteorological Society, 100, 137–153, https://doi.org/10.1175/BAMS-D-17-0165.1, 2019.

Wainwright, C. E., Bonin, T. A., Chilson, P. B., Gibbs, J. A., Fedorovich, E., and Palmer, R. D.: Methods for evaluating the temperature structure-function parameter using unmanned aerial systems and large-eddy simulation, Boundary-Layer Meteorology, 155, 189–208, 2015.

Zhang, Y. and Klein, S. A.: Mechanisms affecting the transition from shallow to deep convection over land: Inferences from observations of the diurnal cycle collected at the ARM Southern Great Plains site, Journal of the Atmospheric Sciences, 67, 2943–2959, 2010.

Zielke, B.: A Procedure for Obtaining High-Density In-Situ Measurements of Ozone Concentration Within the Planetary Boundary Layer, Master's thesis, University of Oklahoma, 2011.